

# Direct Georeferencing for Portable Mapping Systems: In the Air and on the Ground

Lasse Klingbeil <sup>1</sup>, Christian Eling <sup>2</sup>, Erik Heinz <sup>3</sup>,  
Markus Wieland <sup>4</sup>, Heiner Kuhlmann <sup>5</sup>

## ABSTRACT

During the last years, the acquisition of geometric information about objects by using a moving sensor platform, has gained an increasing popularity in the surveying community. On the one side, a large number of companies offer vehicle-based mobile mapping systems, which usually contain a fast profile laser scanner, a high precision Inertial Measurement Unit and geodetic GNSS receivers in order to directly georeference the laser scans and build a consistent point cloud of the object. On the other side there are a growing number of companies, offering small and lightweight Unmanned Aerial Vehicles (UAVs), which automatically fly over the area of interest and create dense point clouds of the environment by using camera images and photogrammetric processing software. In this case, the georeferencing is usually realized by ground control points. This contribution summarizes the activities of the authors to bring both fields closer together by developing a small (11 cm x 10 cm x 5 cm) and lightweight (240 g) direct georeferencing unit, which is able to provide accurate position ( $< 5$  cm) and orientation ( $< 1^\circ$ ) information in real time. We describe the development of the sensor unit and the sensor fusion algorithms, address the topics of calibration and accuracy evaluation, and we provide an overview of different applications, where the unit has been already used. These include the high resolution acquisition of crop surface models by using UAV based imagery, the direct georeferencing of an autonomously flying robot with a laser scanner and multiple cameras, and the generation of laser point clouds using a human carried mobile mapping system.

---

<sup>1</sup>Senior Research Scientist, Institute of Geodesy and Geoinformation, Rheinische Friedrich-Wilhelms-Universität Bonn, Germany, klingbeil@igg.uni-bonn.de

<sup>2</sup>Research Scientist, Institute of Geodesy and Geoinformation, Rheinische Friedrich-Wilhelms-Universität Bonn, Germany, eling@igg.uni-bonn.de

<sup>3</sup>Research Scientist, Institute of Geodesy and Geoinformation, Rheinische Friedrich-Wilhelms-Universität Bonn, Germany, heinz@igg.uni-bonn.de

<sup>4</sup>Research Engineer, Institute of Geodesy and Geoinformation, Rheinische Friedrich-Wilhelms-Universität Bonn, Germany, wieland@igg.uni-bonn.de

<sup>5</sup>Full Professor, Institute of Geodesy and Geoinformation, Rheinische Friedrich-Wilhelms-Universität Bonn, Germany, heiner.kuhlmann@uni-bonn.de

Keywords: direct georeferencing, UAV, mobile laser scanning, mobile mapping, portable system

This material may be downloaded for personal use only. Any other use requires prior permission of the American Society of Civil Engineers. This material may be found at <https://ascelibrary.org/doi/10.1061/>

Klingbeil, L., Eling, C., Heinz, E., Wieland, M. (2017): Direct Georeferencing for Portable Mapping Systems: In the Air and on the Ground, J. Surv. Eng., 143(4): 04017010.

## INTRODUCTION

Mobile Mapping has become a popular topic in recent years. In this article, we consider 'Mobile Mapping' as the acquisition of arbitrary spatially distributed information on the basis of a moving sensor platform. In most cases these are geometric data, such as point clouds or derived products, but there are often augmented by radiometric data, such as colors or other spectral information. In this context we also consider aerial photogrammetry as a mobile mapping technology. Many images are taken while the vehicle is flying through or over the area of interest, and later processed to point clouds and other products. By this means, there is no general difference to the 'classical' mobile mapping systems, consisting of a laser scanner and a GNSS/IMU ('Global Navigation Satellite System'/'Inertial Measurement Unit') combination. The challenges are still the accurate trajectory estimation of the platform and the spatial and temporal synchronization of the multi-sensor system (calibration and time synchronization). In mobile laser scanning the trajectory estimation and the georeferencing of scanner data is usually realized using high performance Inertial Measurement Units (IMU) in combination with geodetic grade GNSS receiver (based on differential carrier phase observations). In aerial photogrammetry, the trajectory estimation is part of the bundle adjustment process, where the exterior parameters (rotation and position) of the camera are estimated. The georeferencing is usually realized indirectly by integrating known markers (GCPs, Ground Control Points) into the adjustment process. Although direct georeferencing of aerial images has been realized many years ago, by using the same high performance IMU/GNSS systems, these are not applicable in lightweight unmanned aerial vehicles (UAV), which have become tremendously popular in recent years. This is due to the IMU/GNSS systems high weight and high costs. This paper summarizes the development of a compact direct georeferencing system and its application on different platforms for different tasks. The system was developed to be lightweight and small enough for UAV borne operation, provides high precision position ( $< 5\text{ cm}$ ) and rotation ( $< 1^\circ$ ) information in real-time and enables time synchronization of all sensor data using the GPS (Global Positioning System) PPS-signal (Pulse Per Second). All software components (system control, GPS processing and sensor fusion) have been developed in house in order to achieve a maximum flexibility and to be able to focus on robust and fast GPS ambiguity resolution in non-ideal environments and to incorporate other sensors, such as cameras into the trajectory estimation.

We give an overview of the development of the system and the algorithms (details have been published elsewhere, e.g. in (Eling et al. 2014a; Eling et al. 2014b)) and we demonstrate its functionality in various applications and analysis (which partly have been published elsewhere). Firstly, it is used to measure temporal geometrical changes with UAV based imagery without the use of ground control points. Secondly, it is used as a part of an airborne mobile mapping system, which additionally consists of multiple cameras and a laser scanner, and which is intended to fly fully autonomous and to perform mapping tasks in obstructed areas. Thirdly, the sensor unit is combined with low cost laser scanner, which can be carried by hand to create georeferenced point clouds on the fly.

### A SMALL LIGHTWEIGHT DIRECT GEOREFERENCING SYSTEM

We defined certain goals for the development of a customized direct georeferencing unit. First of all, it had to be small and light-weight, in order to be carried by small UAV ( $< 5kg$ ) without decreasing its payload too much. At the same time, it had to provide a similar functionality as conventional high precision GNSS/IMU systems: accurate absolute position ( $< 5cm$ ) and orientation ( $< 1^\circ$ ) data at high rates (100 Hz) and in real-time, precise time stamping of measurements and events using the GPS PPS (pulse-per-second) signal, bridging non-ideal GNSS condition by integrating IMU or other sensor data using advanced sensor fusion algorithms. For the latter it was important to have access to all raw sensor measurements, including GNSS carrier phase observations. One of our research goals was the development of robust and fast GPS carrier phase ambiguity resolutions, enabling RTK (Real Time Kinematik) GPS processing, even in demanding conditions. We also wanted to be able to integrate other sensing modalities, such as multi-camera systems, into the trajectory estimation process. Therefore all algorithms, starting from the low level GNSS processing up to the sensor fusion has been developed in house.

Fig.1 (a) shows a prototype of the sensor unit. The sensor and processing components of the unit and the data flow is shown Fig.1 (b). The main positioning device is a Novatel OEM615 dual frequency GPS receiver. A second GPS receiver (single frequency, ublox) enables the realization of a very short baseline on board of the UAV, which can be used to derive heading information. A tactical grade MEMS (Microelectromechanical Systems) IMU (Analog Devices 16488) provides inertial sensor data (acceleration and angular rate), magnetic field measurements and barometric pressure information. A radio module is used to receive GPS observations from a master station, which is necessary for RTK mode GPS processing. All these data sources are connected to an FPGA (Field Programmable Gate Array), which is part of a general purpose Input-Output Board (National Instruments sbRIO 9696) containing also a processor with a Real-Time Operating System (RTOS). The FPGA in combination with the RTOS enables fast parallelization of serial data streams and a time deterministic acquisition and processing of the sensor readings. The internal system clock of the processor is synchronized with the PPS signal from the GPS receiver, which enables precise time stamping.

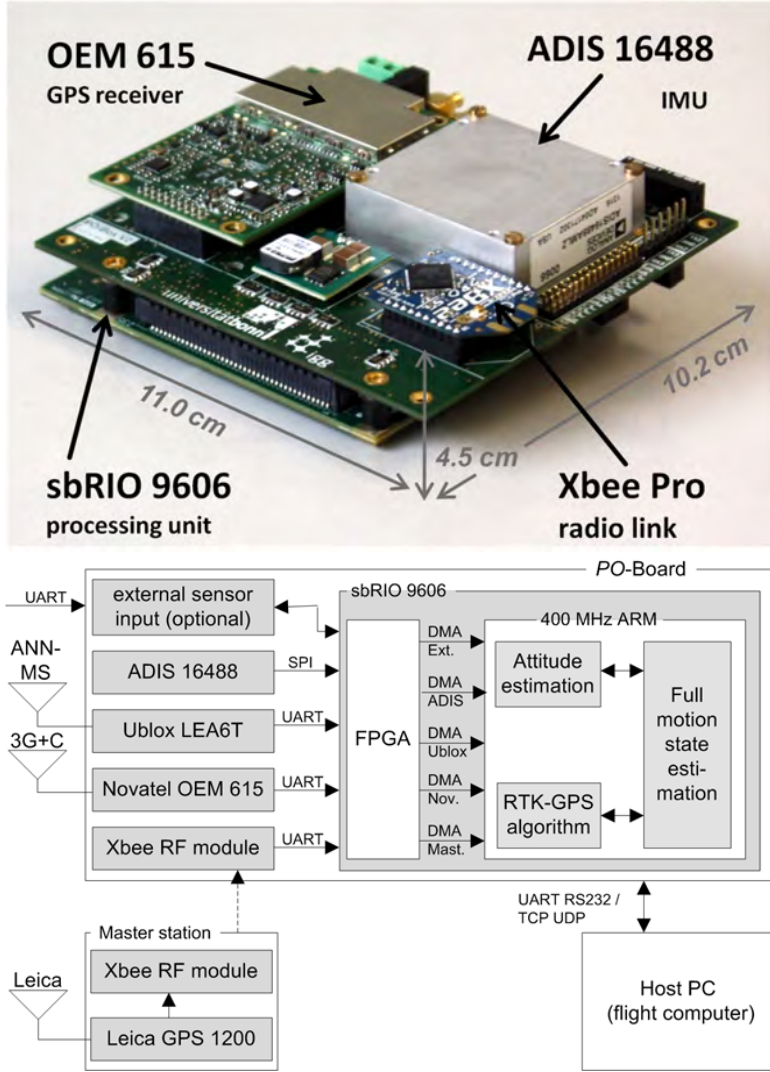


FIG. 1. Direct Georeferencing Unit: (a) Photo and (b) block diagram.

ping and synchronization of events, such as the image exposure as shown later in Section 3. There is also the option to integrate other sensors as laser scanners, as shown in Section 3. The unit has a size of 11 cm x 4.5 cm x 10.2 cm and a weight of 240 g including two geodetic grade antennas. For this, the antennas have been disposed of their casing and then recalibrated in our anechoic chamber (Zeimetz and Kuhlmann 2010).

The sensor fusion algorithms to provide position and orientation estimation are realized as tasks on the real-time processor. The accelerometer and gyroscope readings are integrated using a classical strapdown integration approach. The integration error is estimated using an Extended Error State Kalman Filter (EEKF) with errors in position  $p^e$ , velocity  $v^e$ , orientation  $\psi$ , accelerometer bias  $\mathbf{b}_a^b$  and

gyroscope bias  $\mathbf{b}_\omega^b$  as state vectors:

$$\delta \mathbf{x} = [\delta \mathbf{x}_p^{e,T} \quad \delta \mathbf{v}_{eb}^{e,T} \quad \delta \psi^T \quad \delta \mathbf{b}_a^{b,T} \quad \delta \mathbf{b}_\omega^b{}^T]. \quad (1)$$

The errors are fed back to the strapdown integration task in closed loop manner, whenever an update of the filter is available. The following observations are used to update the Kalman Filter:

**GPS positions** The GPS processing tasks receives dual frequency carrier phase observations from the GPS receiver with a frequency of 10 Hz. It also receives observations via the radio module from the master station whenever they are available. Based on these data, a GPS solution is calculated. Depending on the data availability, the satellite constellation and other environmental conditions, this solution may be a code based solution ( $\sim 3 - 5 m$  accuracy), a float solution ( $\sim 50 cm$  accuracy) or a fixed solution ( $\sim 1 - 3 cm$  accuracy). Details on the RTK processing and the ambiguity resolution can be found in (Eling et al. 2014b).

**Magnetometer** The magnetometer provides an absolute heading reference, however it may be heavily disturbed due to ferromagnetic materials on the UAV and due to strong DC currents of the engines. Therefore it is used only with low confidence.

**Onboard baseline parameters** A short single-frequency GPS baseline is calculated with a frequency of 1 Hz. This is the vector between the two GPS antennas in a global coordinate system, based on the observations of the two GPS receivers. Since a fast resolution of the carrier phase ambiguities is a difficult task when only single-frequency observations are available, the data from the IMU and the magnetometer are used to support this process (see (Eling et al. 2015a) for details).

In cases where no GPS observations are available, the filter switches to a different mode, where the strapdown integration is paused, because it would drift unbounded due to the missing absolute reference. In these cases no position estimation is possible, but the orientation is still available. It should be noted here, that a so called tightly-coupled approach, where the GPS processing and especially the ambiguity resolution is part of the GPS/IMU integration task, is certainly a desirable option. However, in the current state of the development we decided for a loosely coupled approach for robustness and stability reasons.

The system offers multiple ways to access the data offline or in real-time. For geo-tagging of aerial images, as described in Section 3 the processed trajectory and the times of occurrence of any external event, such as an image exposure, is logged to a USB (Universal Serial Bus) stick for further offline processing. In the case of the autonomous flight (Section 3), where the trajectory information is used in real-time for path planning and obstacle avoidance, an Ethernet interface

provides messages to any host PC (Personal Computer), even in the form of a standard ROS (Robot Operating System (Quigley et al. 2009)) message, which is very popular in the robotics community, especially for distributed autonomous systems. A RS232 interface also provides the position and orientation data in a form, which may be readable by any autopilot systems.

As for any other multi-sensor system, a system calibration procedure has to be applied, determining the transformations (position and orientation) between all sensors. An example of the calibration between the mapping sensor and the georeferencing unit is given later in the section 'portable laserscanning'. The vector between the GNSS antenna and the IMU is measured physically. The transformations between the inertial sensors are considered to be known, since the IMU is a closed factory calibrated system. The scale factors and cross axis sensitivities of all inertial sensors are also taken from factory calibration and the sensor offsets are estimated on the fly as part of the state vector.

An experimental validation of the position and orientation estimation quality of the system is difficult, since an independent system with a significantly higher accuracy is not available for the typical operation environment of the device. To validate the orientation accuracy, we attached the georeferencing system to a very high precision fiber optic gyro based IMU. The whole system was moved around in order to simulate flight trajectories, and the orientation output of the IMU has been logged to compare it with our solution. Fig 2 shows the difference of both solutions. Given the quality of the IMU and the relatively short measurement time, we consider the IMU solution to be error free. The error of our solution is always below half a degree, in both static and dynamic motion cases, and the roll and pitch errors are even smaller. More on this investigation and on the orientation estimation algorithms can be found in (Eling et al. 2015a).

The position validation and the general functionality of the system is demonstrated indirectly in the next sections by presenting a number of applications, where the unit has been successfully used.

It should be noted here, that especially in cases where the position and orientation solution is used in real-time for control purposes, proper quality-control methods are necessary to ensure the integrity of the system. As described in (Hewitson and Wang 2010) or (Wang et al. 2012), there are various methods, based on GNSS RAIM (Receiver Autonomous Integrity Monitoring) procedures, which have been extended to work with GNSS/IMU systems. This is not part of the current research and beyond the scope of this paper, however, as a crucial component of real-time navigation it is mentioned and considered as future work.

## APPLICATIONS

### Measuring changes

One application of Mobile Mapping Systems is the detection and analysis of changes of the geometrical appearance of an environment or object between two or more measurement epochs. These can be changes of the earth surface due to geological or geomorphological processes, changes of the geometry of man made

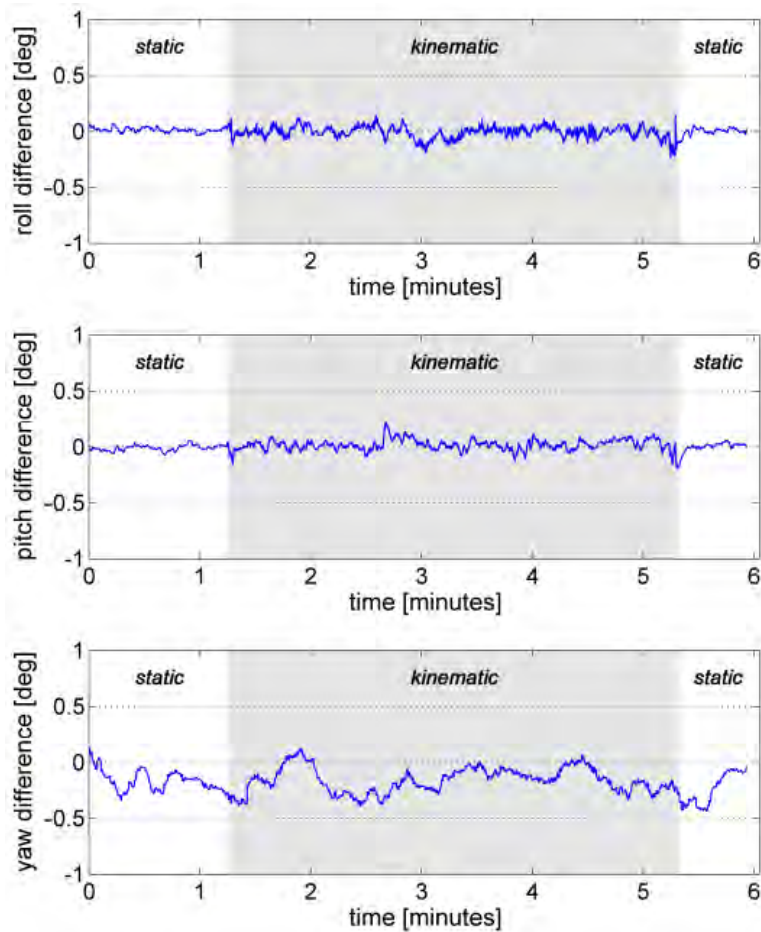


FIG. 2. Estimation error of the georeferencing unit with a very high performance IMU as reference.

objects, such as dams or bridges, but also changes of the phenological status of plants, such as as the plant height in a wheat field during the growing season. A 3D data set (e.g. a point cloud) of the object of interest is usually acquired for each epoch using the mobile mapping system. For data analysis, the data sets of each epoch have to be registered to be in the same coordinate system. This can be realized by known static points, such as GCPs, by registration of unchanged areas using ICP (iterative closest points (Besl and McKay 1992)) or by direct georeferencing, where the point cloud for every epoch is independently referenced using GNSS observations. The usage of a small UAV as mobile mapping system, with a consumer grade camera as a sensor and a direct georeferencing unit for registration of data sets from different epochs is presented here. The UAV is shown in Fig. 3. It is based on a Mikrokopter OktoXL (HiSystems GmbH) and contains a Panasonic Lumix GX1 16MPixel consumer camera, as well as the direct georeferencing system described above. An important feature of the system

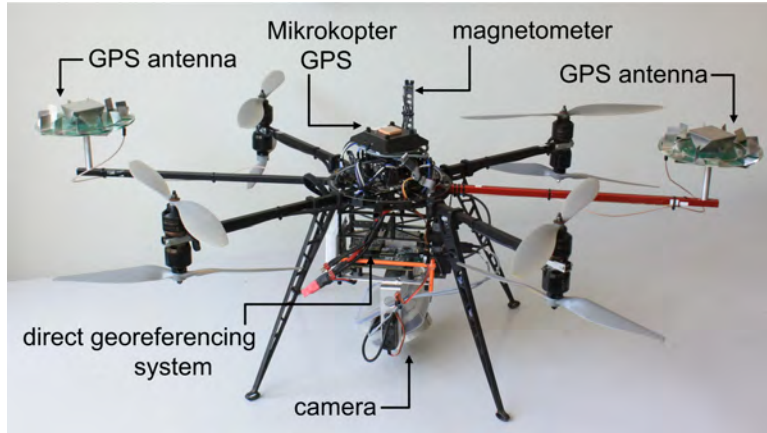


FIG. 3. UAV for directly georeferenced aerial photogrammetry.

is the synchronization of the camera images and the position and orientation information. Depending on the velocity of the UAV, an uncertainty of the actual moment of exposure in the order of a few milliseconds can lead to significant uncertainties in the estimated image position. Some cameras offer a reliable signal, which is perfectly synchronized with the moment of exposure, but most of them don't. In our case we had to tap an internal camera signal in order to get the correct event. Details on the camera synchronization can be found in (Eling et al. 2015b).

The work-flow of our system to get a georeferenced point cloud is the following (see 4): First, we generate a flight path for the UAV, which is defined by the area of interest and the desired ground resolution of the images. While the UAV flies along this predefined path, it constantly takes images with the camera pointing downwards (frequency 1-2Hz). The signal, which indicates the actual moment of exposure is fed into the georeferencing unit and logged as a time stamp in the GPS based time system. Furthermore the positions and attitudes of the UAV at these image time stamps are calculated. After the flight, the images and the image positions are processed using a commercially available photogrammetric processing software (we use both, Agisoft Photoscan and Pix4D Mapper). These software packages align all images using bundle adjustment algorithms and then use the camera positions to georeference the whole image bundle. They also calculate a dense point cloud based on the sparse point cloud resulting from the image alignment. This dense georeferenced point cloud with a point distance in the order of a few millimeters is the final result of the measurement process. It should be noted, that due to the nature of the photogrammetric algorithms, only objects with sufficient texture lead to reconstructable points on their surfaces. Point clouds from different epochs are now compared and analyzed using deformation analysis or change detection methods.

Fig.5 (b) shows the difference between a point cloud created as described

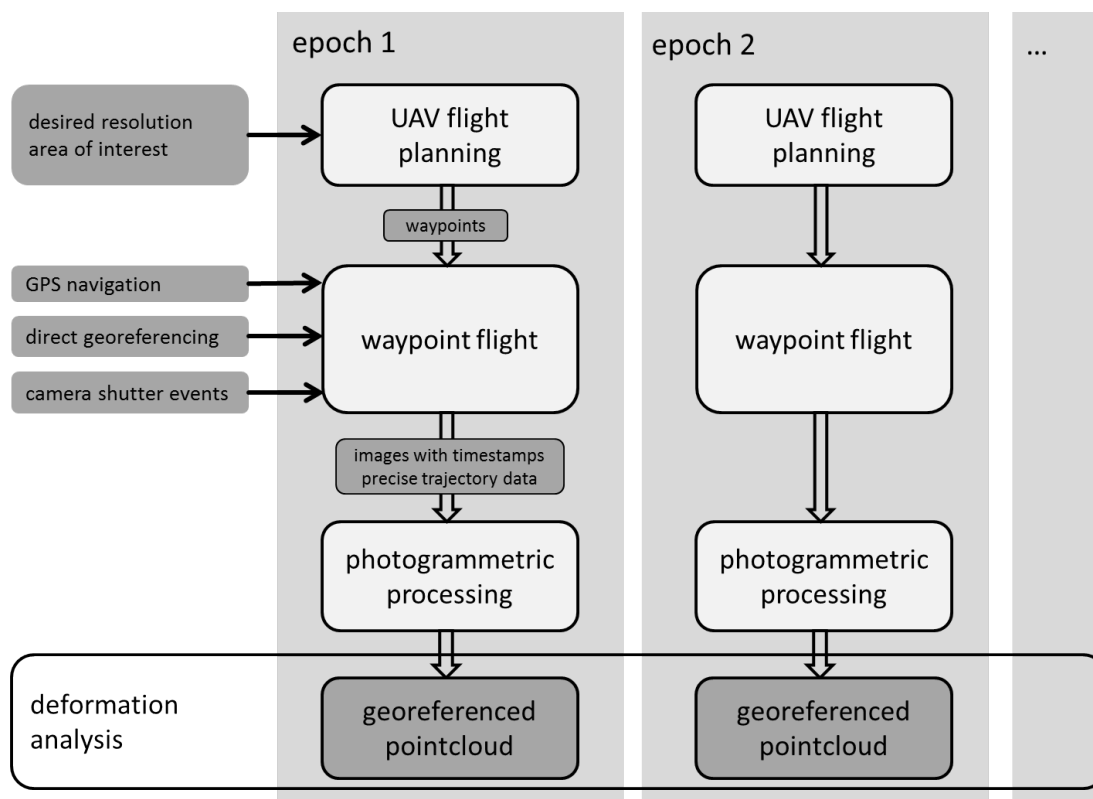


FIG. 4. Workflow for deformation analysis.

above (not using any ground control points), and a point cloud created by a terrestrial laser scanner (Leica P20). The latter has been georeferenced using scanner targets. The difference is calculated as a nearest neighbor point to point distance. The test field is placed on an agricultural field and contains various cylinders and flat surfaces (Fig.5 a). It can be seen, that most of the area shows a difference in the order of 1 cm, which is in the order of the expected GPS accuracy. The brighter areas ( 3 cm) can be recognized as footsteps, which has been left on the ground (agrarian soil) by the person placing the laser scanner at three different spots. This figure demonstrates the general functionality of the direct georeferencing of UAV imagery and its integration into the photogrammetric point cloud generation process. To simulate a deformation process, we slightly changed the test area between two measurement epochs by bending one of the flat surfaces, rotating the cylinders and the other flat surface for a few degrees around different axis and by piling up some of the soil. The point to point distance between the two independent directly georeferenced photogrammetric point clouds is shown in Fig. 5 (b). The deformations can be clearly seen. There are also other footsteps visible now, coming from the activities while changing the test area. More details on this investigation can be found in (Eling et al. 2016).

The accuracy of the georeferencing on the UAV can be seen in Fig. 6. Here

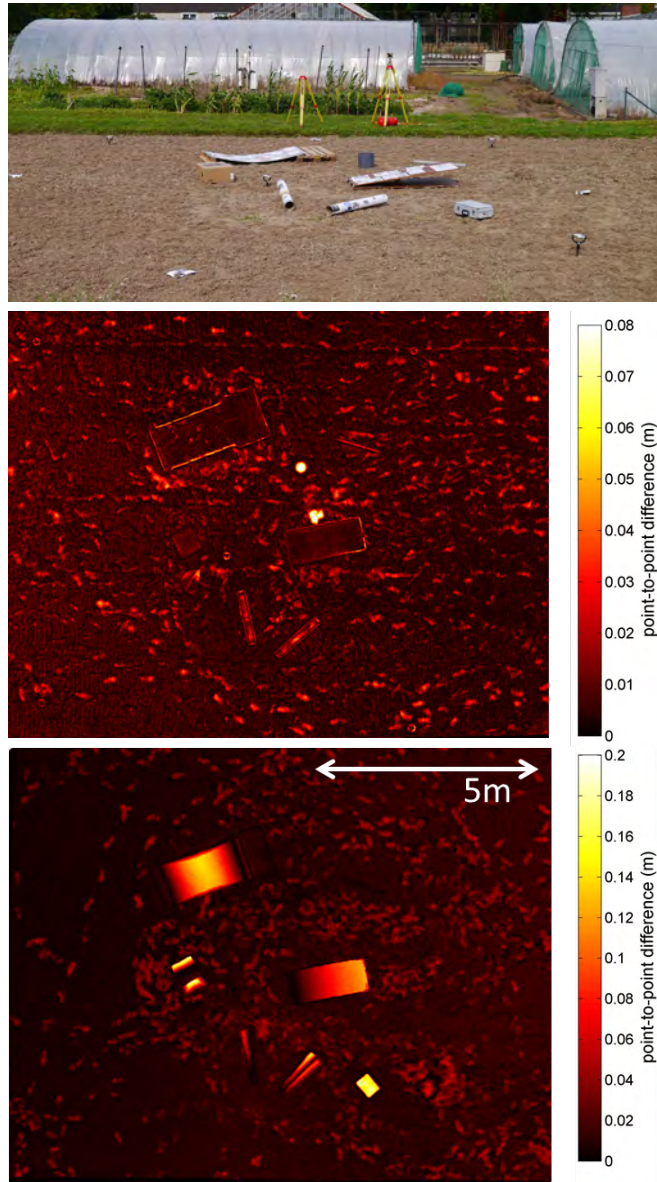


FIG. 5. (a) Test area on an agricultural field. (b) Point to point distances between a directly georeferenced photogrammetric point cloud (no GCPs) and georeferenced terrestrial laser scan (with GCPs) of the test field (top view). (c) Point to point distance between two independent directly georeferenced photogrammetric point clouds from two measurement epochs with simulated deformation (top view).

the bundle adjustment has been performed using precisely measured ground control points and not using the information from the direct georeferencing system. The camera positions from this bundle adjustment have been compared with the positions provided by the direct georeferencing unit. The differences are in the

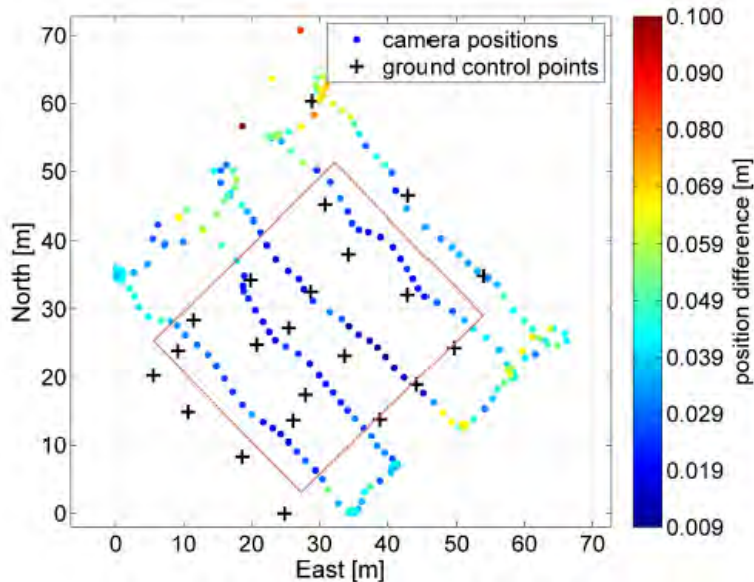


FIG. 6. Georeferencing accuracy estimated based on bundle adjustment.

order of a few centimeters in the area where a sufficient number of GCPs is available. Although it is not clear from the plot, where the difference comes from, the systematic deviations at the edges of the area are assumed to be caused by the bundle adjustment, resulting from the image geometry at the edges and from the estimation of the internal camera parameters. See (Eling et al. 2015b) for more details on this investigation.

A series of applications of this method can be found in the area of agriculture, more precisely within a topic called 'Precision Agriculture'. In simple words, this is a farming management concept based on observing, measuring and responding to inter and intra-field variability in crops. In this context, we concentrate on the observing and measuring part, which can be done using UAVs in many ways. While some researchers acquire radiometric information using multi-, hyper-spectral or thermal cameras to extract indicators for example photosynthesis activity or other phenological traits (e.g. (Turner et al. 2014; Candiago et al. 2015)), we concentrate on geometrical features, such as the plant height. Using directly georeferenced point clouds from a crop field at two different epochs, we can extract the growth rate of the plant with a high spatial accuracy. An example is shown in Fig.7 where the height difference of a wheat field between two weeks of growth is shown. The high spatial resolution allows the mapping of the data to certain crop variants, which are organized in small plots in this example.

It should be noted here, that this difference could have been easily calculated without any georeferencing, simply by leaving some markers on the ground, which later could be used to register the point clouds from the two measurement

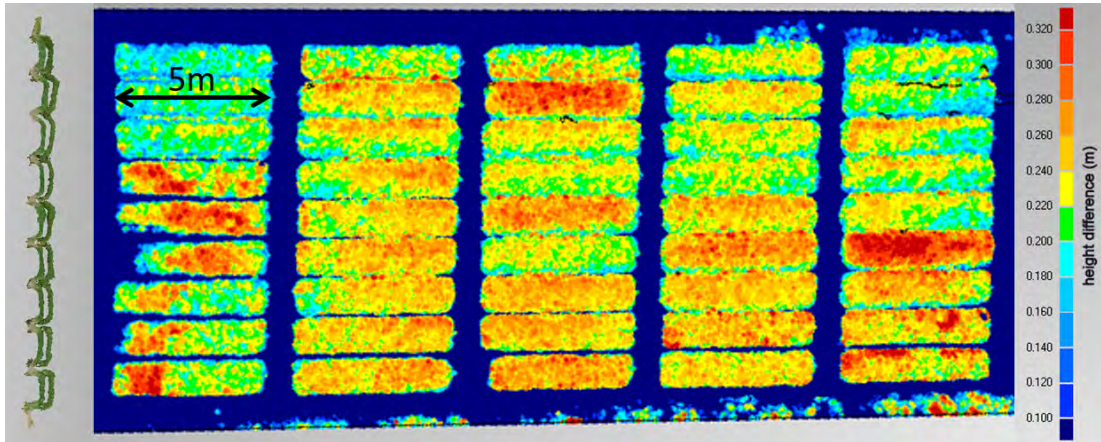


FIG. 7. Plant height difference in a wheat field between a growth period of two weeks. On the left a cut through both point clouds (side view) is shown.

days. However, the major advantage of our system is, that no preparation of the environment is necessary at all. Although this wouldn't be a problem for most applications, there are certainly situations, where the area is not accessible at all or where the permanence of the ground control points or other recognizable markers can not be guaranteed.

#### Mapping on Demand

Within the project 'Mapping on Demand', partners from Geodesy, Photogrammetry, Computer Science and Robotics work together to develop and test a lightweight autonomously flying UAV that is able to identify and measure inaccessible three-dimensional objects using visual information. A major challenge within the project comes with the term 'on demand'. Apart from the classical 'mapping' part, where 3D information is extracted from aerial images as described above, the UAV is intended to fly fully autonomous on the basis of a high-level user request, avoiding obstacles and processing mapping data in real-time including the extraction of semantic information. Therefore a precise and robust direct georeferencing is necessary, not only for the real-time processing of the image data, but also for the autonomous navigation of the system. Fig. 8 shows one of the vehicles, that have been developed within the project.

Its basic setup is similar to the one already presented above, however its sensing and processing capabilities are much higher due to the complex task it has to fulfill. Apart from the already presented direct georeferencing system with its two antennas and the external magnetometer, it also contains two stereo camera systems with 180° fish-eye lenses, and an Ethernet connected industrial camera, replacing the consumer camera of the previous setup. The UAV also contains an up-to-date quad core processor board, which is mainly used for the image processing and path planning. A WLAN (Wireless Local Area Network) interface enables a constant connection to a ground station, which is used for

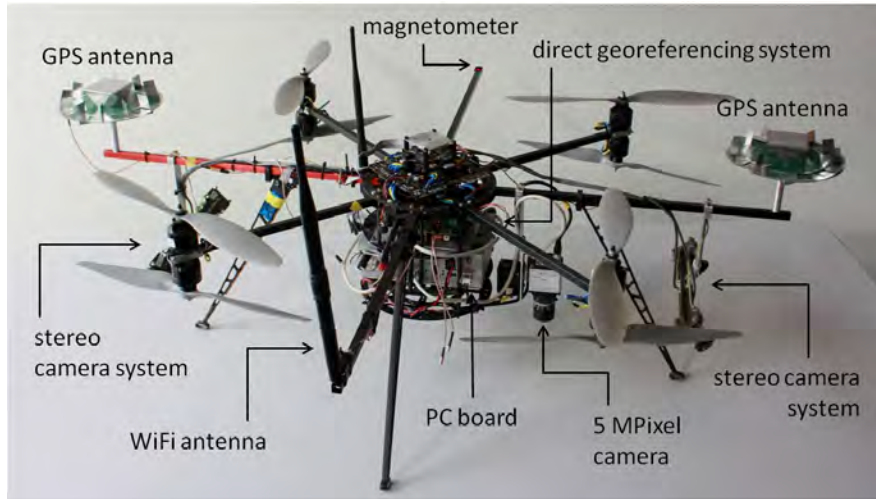


FIG. 8. UAV used for autonomous flight and mapping of buildings.

system monitoring and image streaming. An other version of the UAV, which is not shown here, also contains a small rotating profile laser scanner, which is used for obstacle avoidance (Droeschel et al. 2014). An overview of the contributions of each project partner can be found in (Klingbeil et al. 2014), here we only give a short summary, related to the direct georeferencing unit.

The work flow of the mapping system, as it is currently under development, is sketched in Fig. 9. On the basis of the high rate real-time position and orientation information coming from the sensor unit presented above, the UAV navigates through the environment. It also uses current sensor readings from the laser scanner and the cameras to avoid obstacles. It also includes information from external available maps or previous mapping missions into the flight planning process. Because the georeferencing mainly relies on the GPS, which can easily be disturbed in areas with buildings and trees, the four stereo cameras are also used as trajectory estimation sensors. The optical trajectory estimation ('visual odometry') is based on consecutive resection steps at the image frame rate (10 Hz) and an incremental bundle adjustment on selected keyframes (Schneider and Förstner 2014; Schneider and Förstner 2013). GPS information from the georeferencing unit are also integrated into the estimation process whenever they are available, to define the global coordinate system and to avoid long term drift effects of the bundle adjustment (Schneider et al. 2016).

This incremental bundle adjustment, including its trajectory and a sparse point cloud is not available in real-time, due to the high computational costs of the image processing, but it still provides data with a delay of a few seconds. Therefore the data are not used in the low level control loop of the UAV, but they can be used as a backup in cases of GPS outage and they provide a higher orientation accuracy than the IMU based estimation from the georeferencing

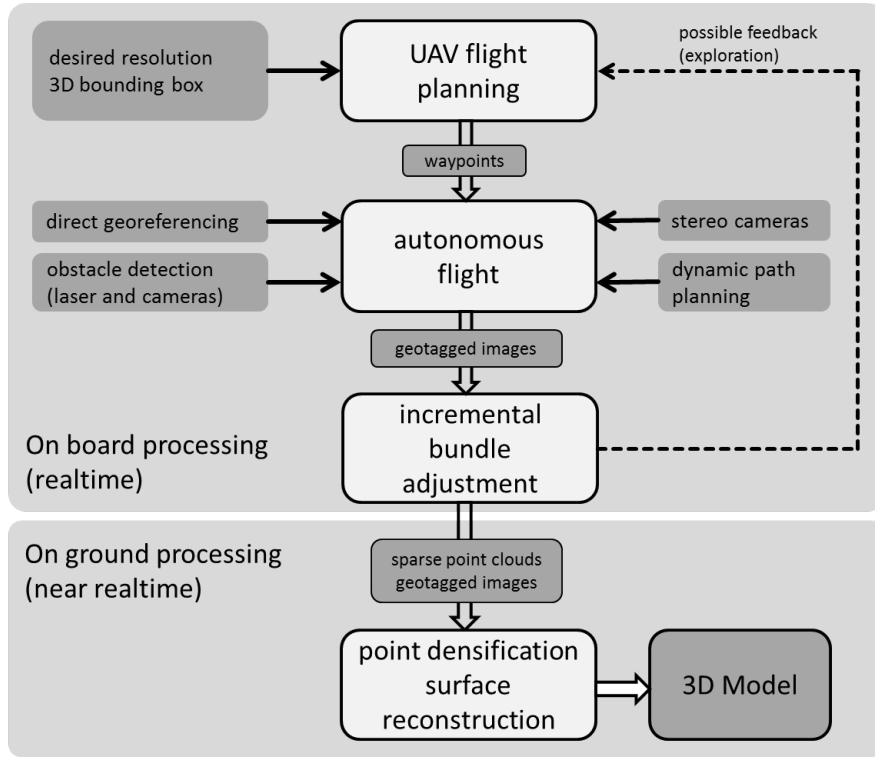


FIG. 9. Workflow for the Mapping on Demand application.

unit. The poses from the incremental bundle adjustment are also used to tag the higher resolution image from the main camera on the UAV, which is later used to generate point clouds and reconstruct object surfaces. Fig. 10 shows the union of three georeferenced point clouds which have been calculated based on images recorded during three different flights. The back of the building was observed during one flight and the front and side was seen during two other flights. The compatibility of the clouds demonstrate the general functionality and the advantage of the direct georeferencing compared to methods, where GCP or other known landmarks have to be used. In this case the point cloud densification was performed off-line using the freely available software package PMVS2 (Furukawa and Ponce 2010).

#### Portable Laserscanning

In a third application example the direct georeferencing system is used in combination with a profile laser scanner. This resembles the classical mobile mapping approach, where a scanner is moved while scanning the environment and the position and orientation information from an IMU/GNSS combination is used to transform each scan point into one global coordinate system. The sensor system is shown in Fig. 11. It has a total weight of 8.5kg, although the actual weight of the scanner, the georeferencing unit including the antennas and the



FIG. 10. Georeferenced point cloud of a building and surrounding vegetation. The cloud is actually the union of three clouds generated from images from three different flights.

power supply is only about 1kg. The setup here has not been optimized for low weight, but for maximum flexibility and modularity.

The scanner is a Hokuyo UTM-30LX-EW, which is a compact 2D time-of-flight scanner with a  $270^\circ$  field of view,  $0.25^\circ$  angular resolution, 30 m maximum (guaranteed) range and 40Hz scanning rate. Its main characteristics are the small dimensions (62 mm x 62 mm x 87.5 mm) and the low weight (210 g, without cable). It is mounted in a way, that it records vertical profiles.

During the scanning process, every revolution of the scanning mirror generates an electrical signal, which is connected to the FPGA on the georeferencing unit. Here the signal is time stamped using the GPS time base and the scanner observations are transferred to the processor using an Ethernet interface. By linear interpolation between two revolution time stamps every single scan point is mapped to a certain position and orientation of the sensor system and thus transformed to the global GPS coordinate system. Thus, the georeferenced point cloud is generated in real-time on board of the georeferencing unit.

A crucial point in the process of the point cloud generation is the calibration of the sensor system, meaning the determination of the usually time independent transformation between the laser scanner and the georeferencing unit. As shown in Fig. 12 (a) and described in more detail in (Heinz et al. 2015) the calibration

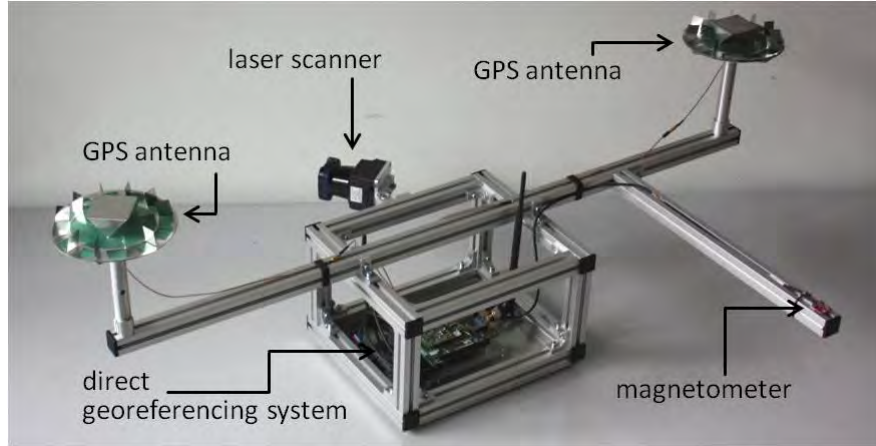


FIG. 11. Portable system consisting of the georeferencing system and a light-weight profile laser scanner.

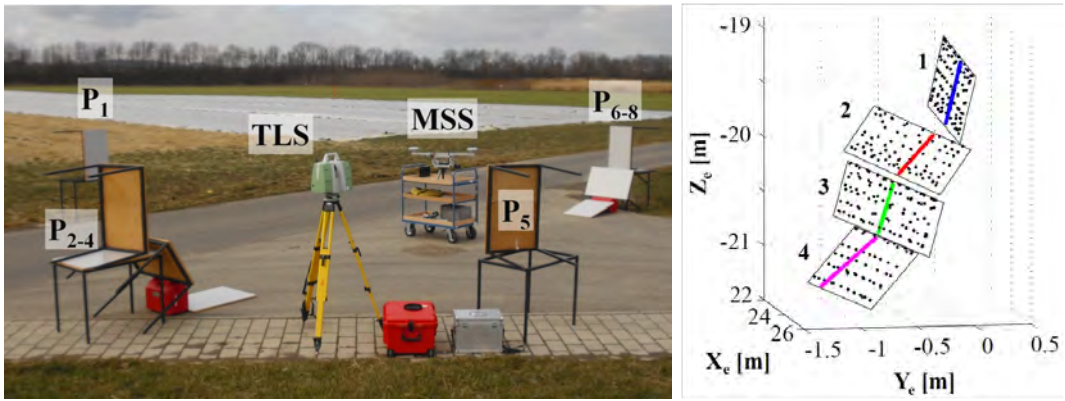


FIG. 12. (a) calibration setup. (b) TLS scan points on the planes and scan lines from the Hokuyo scanner.

process is based on eight differently oriented flat surfaces  $P_1 - P_8$ , which have been accurately measured and georeferenced using a terrestrial laser scanner (TLS). The TLS has been localized in the global GPS coordinate system by using ground control points. The required transformation is then estimated by comparing the Hokuyo scan lines, transformed using the poses from the georeferencing unit, with the surface parameters, which have been extracted from the TLS scan (Fig. 12 b). This methods led to calibration accuracies of a few millimeters for the lever arm and about  $0.1^\circ$  for bore-sight angles. These values are consistent with expected accuracy of the scanner ( $\sim 1-3\text{cm}$ ) and the georeferencing system ( $< 5\text{cm}$ ,  $< 1^\circ$ ). An analysis has shown, that based on the quality of this calibration and on the stochastic properties of the sensor observations, a point accuracy of about 4 cm, 6 cm, 12 cm and 18 cm in the distance range up to 5 m, 10 m, 20 m and 30 m

respectively can be expected. This could also be verified by comparison of a mobile scan with a static terrestrial reference scan of a building (Heinz et al. 2015).



FIG. 13. Directly georeferenced point cloud of a building. The points were generated in real-time without any post processing.

Fig. 13 shows a point cloud, which has been taken while slowly moving along the facade of the building. The point cloud is generated in real-time on the direct georeferencing unit and has not been post-processed in any way. The measurement took only a few minutes. The quality and inner consistency of the resulting point cloud demonstrate the general functionality of the direct georeferencing system, especially regarding the orientation estimation and the time synchronization. Although the point density and the accuracy of the system is not as high as with terrestrial scanners or an up-to-date mobile mapping system, the fast acquisition time and the lack of any post-processing needs, may make it attractive for many applications.

There is also potential for increasing the accuracy by utilizing the actual scanner data as a sensor for the trajectory estimation. While in most mobile mapping systems (as the one presented in this section) the trajectory estimation and the scanning are independent (although time synchronized) processes, it is also possible to use the scanner data as an additional input to the position and orientation algorithms. In the robotics community this concept is well known as SLAM (Simultaneous Localization and Mapping, see e.g. (Thrun et al. 2005)), the incremental bundle adjustment mentioned in Sec. 3 is following the same principle. Especially the robustness and accuracy of the heading angle, which is the most weakly observed parameter, may benefit from this approach.

## CONCLUSIONS AND FUTURE WORK

In this paper we presented a direct georeferencing system, which has been

developed to be lightweight, small and which is able to deliver precise position and orientation information in real-time. We gave an overview of the hardware and software concept of the system and we demonstrated its functionality by a number of different applications.

The system has been used to assign high precision position information to images, taken with a UAV, in order to provide an accurate georeference to the image bundle without any ground control points. The experiments show, that the accuracy of the image tagging is in the order of a few centimeters. By comparing the photogrammetric point cloud with a TLS point cloud, it could be shown, that a similar accuracy could be achieved on the ground. In another application the georeferencing system has been used to provide information to an on-the-fly bundle adjustment process, which again led to georeferenced point clouds of the same accuracy. This time a building was mapped by taking images from the side. In a third example, the unit was combined with a small laser scanner, in order to create a georeferenced point cloud, while moving the device along a building, and without any post-processing. The result also confirmed the centimeter level and sub degree accuracy and the time synchronization capabilities.

Currently, the position and orientation estimation algorithms are being improved further by including other GNSS constellations, such as Glonass, Beidou or Galileo and by including motion information from cameras and laser scanners. A special focus is given to the robustness of the solution in very unpleasant GNSS conditions. We also work on calibration methods for various multi-sensor systems and on systematic methods for their validation.

#### ACKNOWLEDGMENTS

This work was funded by the DFG (Deutsche Forschungsgemeinschaft) under the project number 1505 “Mapping on Demand”. The authors wish to express their gratitude for this support.

#### REFERENCES

- Besl, P. and McKay, N. D. (1992). “A method for registration of 3-d shapes.” *Pattern Analysis and Machine Intelligence, IEEE Transactions on*, 14(2), 239–256.
- Candiago, S., Remondino, F., De Giglio, M., Dubbini, M., and Gattelli, M. (2015). “Evaluating multispectral images and vegetation indices for precision farming applications from uav images.” *Remote Sensing*, 7(4), 4026.
- Droeschel, D., Holz, D., and Behnke, S. (2014). “Omnidirectional perception for lightweight mavs using a continuously rotating 3d laser scanner.” *Photogrammetrie Fernerkundung Geoinformation (PFG)*, 5, 451–464.
- Eling, C., Klingbeil, L., and Kuhlmann, H. (2014a). “Development of an rtk-gps system for precise real-time positioning of lightweight uavs.” *Beiträge zum 17. Internationalen Ingenieurvermessungskurs, Zürich, Wichmann Verlag, Berlin*, 111–123.

- Eling, C., Klingbeil, L., and Kuhlmann, H. (2015a). “Real-time single-frequency gps/mems-imu attitude determination of lightweight uavs.” Sensors accepted for publication.
- Eling, C., Klingbeil, L., Wieland, M., and Kuhlmann, H. (2014b). “Direct georeferencing of micro aerial vehicles - system design, system calibration and first evaluation tests.” PFG - Photogrammetrie, Fernerkundung, Geoinformation, 4, 227–237.
- Eling, C., Klingbeil, L., Wieland, M., and Kuhlmann, H. (2016). “Towards deformation monitoring with uav-based mobile mapping systems.” Proceedings of the 3rd Joint International Symposium on Deformation Monitoring (JISDM), Vienna (March). accepted for publication.
- Eling, C., Wieland, M., Hess, C., Klingbeil, L., and Kuhlmann, H. (2015b). “Development and evaluation of a uav based mapping system for remote sensing and surveying applications.” Int. Arch. Photogramm. Remote Sens. Spatial Inf. Sci., XL-1/W4, 233-239, <<http://www.int-arch-photogramm-remote-sens-spatial-inf-sci.net/XL-1-W4/233/2015/isprsarchives-XL-1-W4-233-2015.pdf>>.
- Furukawa, Y. and Ponce, J. (2010). “Accurate, dense, and robust multi-view stereopsis.” IEEE Transactions on Pattern Analysis and Machine Intelligence, 32(8), 1362–1376.
- Heinz, E., Eling, C., Wieland, M., Klingbeil, L., and Kuhlmann, H. (2015). “Development, calibration and evaluation of a portable and direct georeferenced laser scanning system for kinematic 3d mapping.” Journal of Applied Geodesy, 9(4), 227–243.
- Hewitson, S. and Wang, J. (2010). “Extended receiver autonomous integrity monitoring (eraim) for gnss/ins integration.” Journal of Surveying Engineering, 136(1), 13–22.
- Klingbeil, L., Nieuwenhuisen, M., Schneider, J., Eling, C., Droschel, D., Holz, D., Läbe, T., Förstner, W., Behnke, S., and Kuhlmann, H. (2014). “Towards autonomous navigation of an uav-based mobile mapping system.” Proceedings of the 4th International Conference on Machine Control & Guidance, <<http://www.digibib.tu-bs.de/?docid=00056119>>.
- Quigley, M., Conley, K., Gerkey, B., Faust, J., Foote, T., Leibs, J., Wheeler, R., and Ng, A. Y. (2009). “Ros: an open-source robot operating system.” ICRA workshop on open source software, Vol. 3, 5.
- Schneider, J., Eling, C., Klingbeil, L., Kuhlmann, H., Förstner, W., and Stachniss, C. (2016). “Fast and effective online pose estimation and mapping for uavs.” Proceedings of the IEEE Int. Conf. on Robotics & Automation (ICRA).
- Schneider, J. and Förstner, W. (2013). “Bundle adjustment and system calibration with points at infinity for omnidirectional camera systems.” Photogrammetrie – Fernerkundung – Geoinformation (PFG), 4, 309–321.
- Schneider, J. and Förstner, W. (2014). “Real-time accurate geo-localization of a mav with omnidirectional visual odometry and gps.” ECCV Workshop: Computer Vision in Vehicle Technology, Vol. 8925 of L.N. in Computer Science, 271–282.

- Thrun, S., Burgard, W., and Fox, D. (2005). Probabilistic Robotics (Intelligent Robotics and Autonomous Agents). The MIT Press.
- Turner, D., Lucieer, A., Malenovsky, Z., King, D. H., and Robinson, S. A. (2014). “Spatial co-registration of ultra-high resolution visible, multispectral and thermal images acquired with a micro-uav over antarctic moss beds.” *Remote Sensing*, 6(5), 4003.
- Wang, J., Almagbile, A., Wu, Y., , and Tsujii, T. (2012). “Correlation analysis for fault detection statistics in integrated gnss/ins systems.” *Journal of global positioning systems*, *Journal of global positioning systems*(2), 89 – 99.
- Zeimetz, P. and Kuhlmann, H. (2010). “Validation of the laboratory calibration of geodetic antennae based on gps measurements.” FIG Working Week, 11.-16. April, Sydney, Australia.